IEEE Transactions on Nuclear Science, Vol. NS-30, No. 4, August 1983

REC QUADRUPOLES AND DIPOLES WITH CIRCULAR AND ELLIPTICAL CROSS SECTIONS

R.L. Gluckstern*
Physics Department, University of Maryland, College Park, Maryland 20742
and
R.F. Holsinger
Field Effects, Carlisle, Massachusetts 01741

Introduction

The use of segmented rare earth cobalt (REC) rings to produce high field, high quality quadrupoles to focus charged particle beams[1] is increasing. Current designs are based on the properties of 2-D rings with continuous rotation of the easy axis. Since many applications involve elliptically shaped beams, in this paper we explore the possibility of using elliptically shaped 2-D rings as a means of reaching higher fields with less REC material. After showing that such improvement is possible, we investigate the modifications required by segmentation numerically.

Continuous Rotation of Easy Axis

We start our analysis with a simple derivation† of the multipole behavior for a circular ring of inner radius a and outer radius λa, where the easy axis angle is chosen to be

$$\alpha = (m + 1)\theta + \frac{\pi}{2} . \tag{1}$$

Here m is an integer (m = 1 for dipole, 2 for quadrupole, 3 for sextupole, etc.) and θ is the azimuthal angle. The scalar potential is given, in 2-D, by

$$\Phi(r,\phi) = \frac{1}{2\pi}\int_a^{\lambda a} RdR \int_0^{2\pi} d\theta \frac{\vec{p}\cdot(\vec{r}-\vec{R})}{|\vec{r}-\vec{R}|^2}$$

$$= \frac{p}{2\pi}\int_a^{\lambda a} RdR \int_0^{2\pi} d\theta \frac{(r\cos(\alpha-\phi) - R\cos(\alpha-\theta))}{r^2 + R^2 - 2rR\cos(\phi-\theta)}$$

$$= -\frac{p}{2\pi}\,\mathrm{Re}\int_a^{\lambda a} RdR \int_0^{2\pi} d\theta \left(\frac{e^{i\alpha}}{Re^{i\theta} - re^{i\phi}}\right) \tag{2}$$

where p is the remanant field strength (magnetization per unit area). For $r < R$ the integral can be expanded to obtain the mutlipole series

$$\Phi(r,\phi) = -\frac{p}{2\pi}\sum_{n=0}^{\infty} r^n e^{in\phi}\int_a^{\lambda a}\int_0^{2\pi} RdRd\theta\; e^{i\alpha}(Re^{i\theta})^{-n-1}. \tag{3}$$

The form of easy axis rotation in (1) leads directly to

$$\Phi(r,\phi) = p\,\frac{r^m \sin m\phi}{(m-1)\,a^{m-1}}\left(1 - \frac{1}{\lambda^{m-1}}\right) . \tag{4}$$

The field is then a pure m-pole, with maximum field strength at the bore given by

$$B_m(a) = p\,\frac{m}{m-1}\left(1 - \frac{1}{\lambda^{m-1}}\right) . \tag{5}$$

For m=1, 2, the reduced forms are

$$B_1(a) = p\,\ell n\,\lambda \tag{6}$$

$$B_2(a) = 2p\left(1 - \frac{1}{\lambda}\right). \tag{7}$$

For elliptical rings we start with (3) in the form

$$\Phi(r,\phi) = -p\,\mathrm{Re}\sum_{n=0}^{\infty} r^n e^{in\phi} G_n \tag{8}$$

where

$$G_n = \frac{1}{2\pi}\iint \frac{dx\,dy\,e^{i\alpha}}{(x+iy)^{n+1}} \tag{9}$$

The region of integration in (9) is the cross section of the elliptical ring.

We will choose the geometry of the elliptical ring to be given by

$$1 < w < \lambda \quad , \quad 0 < \psi < 2\pi \tag{10}$$

where

$$x = aw\cos\psi \quad , \quad y = bw\sin\psi \tag{11}$$

Thus, we are choosing similar (rather than confocal) ellipses, with ratio of minor to major axis being b/a, and outer to inner "diameter" being λ. The area element in (9) can now be written as

$$dx\,dy = ab\,w\,dw\,d\psi \tag{12}$$

leading us to

$$G_n = \frac{ab}{2\pi}\int_1^{\lambda}\frac{dw}{w^n}\int_0^{2\pi} d\psi \frac{e^{i\alpha}}{(a\cos\psi + i\,b\sin\psi)^{n+1}} \tag{13}$$

We will now choose

$$\alpha = (m+1)\,\psi + \frac{\pi}{2} \tag{14}$$

and change the variable from ψ to the complex parameter

*Work supported in part by DOE contract AS05-80ER10666.

†The formulation of (1) - (9) for the circular ring parallels that of Halbach in Reference 1.

0018-9499/83/0800-3623$01.00©1983 IEEE

$$z = e^{-i\psi} \quad , \quad d\psi = \frac{idz}{z} \, . \tag{15}$$

The path of integration for z is now the unit circle in the complex plane. Thus we can write

$$G_n = \frac{ab}{2\pi(n-1)} \left(1 - \frac{1}{\lambda^{n-1}}\right) \oint \frac{dz}{z} \frac{z^{-m-1}}{\left[\left(\frac{a}{2}\right)(z + \frac{1}{z}) + \frac{b}{2}\left(\frac{1}{z} - z\right)\right]^{n+1}} \tag{16}$$

where the integration over z is in the counter clockwise direction. If we set

$$\varepsilon = \frac{a-b}{a+b} \tag{17}$$

we can rewrite (16) as

$$G_n = \frac{ab}{2\pi(n-1)} \left(\frac{2}{a+b}\right)^{n+1} \left(1 - \frac{1}{\lambda^{n-1}}\right) \oint \frac{dz\, z^{n-m-1}}{(1 + \varepsilon z^2)^{n+1}} \tag{18}$$

The possible poles of the integrand are at z=0, $\pm i\varepsilon^{-1/2}$. Since $\varepsilon < 1$ for b < a, only the pole at z=0 lies within the unit circle. For m=1 only the term G_1 gives a non-vanishing value. For m=2, only the terms n=0 (constant potential, and therefore not significant) and n=2 give non-vanishing values. For higher values of m contributions come from n=m, m-2, m-4, etc.

We can therefore write

m=1

$$G_1 = iab \left(\frac{2}{a+b}\right)^2 \ell n\, \lambda \qquad G_n = 0 \, , \text{ all other } n \tag{19}$$

and

m=2

$$G_2 = iab \left(\frac{2}{a+b}\right)^3 \left(1 - \frac{1}{\lambda}\right) \qquad G_n = 0 \, , \text{ all other } n > 0. \tag{20}$$

From (8), we obtain the result for the maximum field at the bore (along the x axis, so that r=a).

Dipole

$$B_1 = p \frac{4ab}{(a+b)^2} \ell n \lambda \tag{21}$$

Quadrupole

$$B_2 = p \frac{16a^2 b}{(a+b)^3} \left(1 - \frac{1}{\lambda}\right) \tag{22}$$

We have therefore achieved our desired result, at least for a dipole or quadrupole field; that is, we have provided a prescription for the easy axis rotation (14) which leads to a pure multipole structure for the field.

One of the important consequences of (21) or (22) is that a value of b/a different from 1 leads to a change in the field strength. For example, if λ and a are kept fixed, the dipole field strength in (21) will reduce as b is decreased. For b=a/2, the dipole field strength will be decreased by a factor 8/9, using only half the volume of REC.

For the quadrupole, the field strength actually increases for a while as b is decreased, reaching a maximum enhancement factor of 32/27 for b=a/2. Thus the optimum configuration, involving half the REC volume, produces a maximum quadrupole field

$$B_2(a) = \frac{64}{27} p \left(1 - \frac{1}{\lambda}\right) \, , \tag{23}$$

in contrast with the value in (7) for the circular ring.

Segmented Ring

The analysis of a segmented elliptical ring is far more complex, requiring numerical computation for finite values of ε. The relevant formulas are most directly obtained starting from (9) by changing the scales of x and y and then rotating the axes for each segment. We shall carry through the analysis for N touching trapezoidal segments, as shown in Figure 1 for N=8.

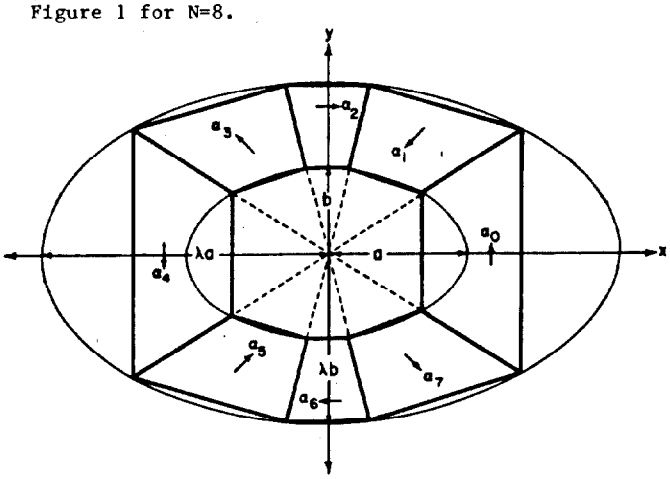

Figure 1. Elliptical Quadrupole With 8 Trapezoidal Segments

Let

$$x = au \quad , \quad y = bv \tag{24}$$

to obtain

$$G_n = \frac{ab}{2\pi} \sum_{j=1}^{N} e^{i\alpha_j} \iint \frac{dudv}{(au + ibv)^{n+1}} \, , \tag{25}$$

where α_j is the (uniform) orientation of the easy axis in the j^{th} trapezoidal segment, as shown in the u-v plane in Figure 2.

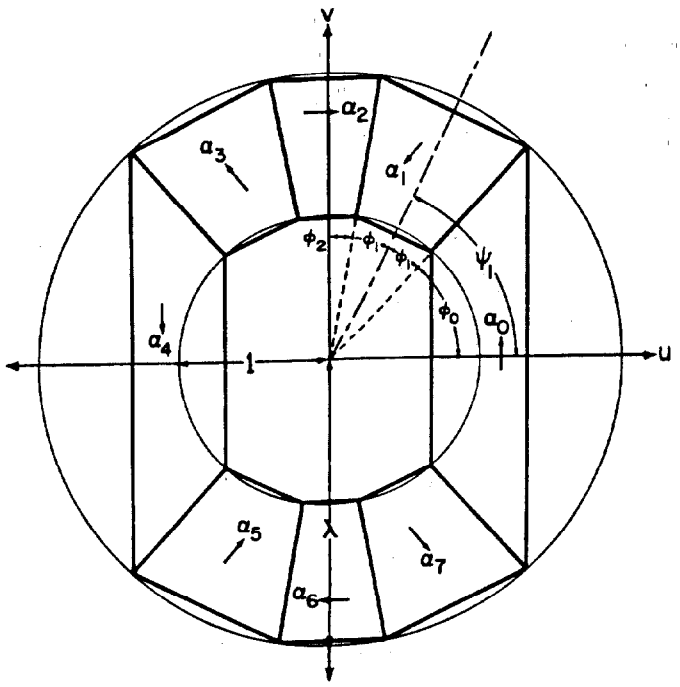

Figure 2. Elliptical Quadrupole With N=8 Transformed to u-v Plane

We will now rotate the j^{th} segment by the angle ψ_j, the mid-angle of the segment, such that

$$u = s\cos\psi_j - t\sin\psi_j$$
$$v = s\sin\psi_j + t\cos\psi_j \qquad (26)$$
$$du\,dv = ds\,dt.$$

This leads to

$$G_n = \frac{ab}{2\pi}\sum_{j=1}^{N} e^{i\alpha_j}\int_{\cos\phi_j}^{\lambda\cos\phi_j} ds \int_{-s\tan\phi_j}^{s\tan\phi_j} dt \;\times$$

$$\frac{1}{[s(a\cos\psi_j + ib\sin\psi_j) + t(ib\cos\psi_j - a\sin\psi_j)]^{n+1}} \cdot \qquad (27)$$

The integrations over t, and then s, can be readily performed, leading to

$$G_n = \frac{ab}{2\pi n(n-1)}\left(\frac{2}{a+b}\right)^{n+1}\left(1 - \frac{1}{\lambda^{n-1}}\right)\sum_{j=1}^{N} Q_j^{(n)} \qquad (28)$$

where

$$Q_j^{(n)} = e^{i\alpha_j}\cos\phi_j\, f\left(\psi_j + \frac{\pi}{2}\right)$$
$$\times\; [f^n(\psi_j - \phi_j) - f^n(\psi_j + \phi_j)] \qquad (29)$$

with

$$f(\beta) \equiv (e^{i\beta} + \varepsilon e^{-i\beta})^{-1} \qquad (30)$$

and

$$f^n(\beta) = [f(\beta)]^n \,. \qquad (31)$$

The multipole component of the field, evaluated at the bore (corresponding to $r = a\cos\phi_o$) is finally

$$B_n(a\cos\phi_o) = p\left(1 - \frac{1}{\lambda^{n-1}}\right) J^{(n)} \qquad (32a)$$

where

$$J^{(n)} = \frac{(1+\varepsilon)^n(1-\varepsilon)\cos^{n-1}\phi_o}{2\pi i(n-1)}\sum_{j=1}^{N} Q_j^{(n)} \qquad (32b)$$

For n=1, one must take the limit as $n \to 1$. Specifically, one has

$$B_1(a\cos\phi_o) = p\,\ell n\,\lambda\,\hat{J}^{(1)} \qquad (32c)$$

where

$$\hat{J}^{(1)} = \lim_{n\to 1}(n-1)\,J^{(n)} \qquad (32d)$$

As a check, it is readily seen, for

$$\varepsilon = 0\,,\quad \alpha_j = \frac{\pi}{2} + (m+1)\psi_j\,,$$
$$\psi_j = \frac{2\pi}{N}j\,,\quad \phi_j = \frac{\pi}{N}\,, \qquad (33)$$

that (32) reduces to (5) multiplied by

$$T_2 = \cos^2\frac{\pi}{N}\;\frac{\sin\frac{2\pi}{N}}{\frac{2\pi}{N}}\,, \qquad (34)$$

Computation

We have written a program which searches for the values of ϕ_j, ψ_j, α_j which lead to the vanishing of

$$J^{(n)},\ n=m+1,\ m+2,\ \ldots\ N+m-1$$

for a variety of values of b/a. Clearly the symmetries shown in Figs. 1 and 2 are appropriate to obtain the proper values in the 2nd, 3rd, and 4th quadrant from those in the 1st quadrant.

Table I-III gives the values of ϕ_j, ψ_j, α_j and $J^{(m)}$ for $\frac{b}{a} = 1.0, .8, .6$, for quadrupoles made up of 8, 16, 32 trapezoidal segments respectively. Tables IV, V give the same information for dipoles for 8, 16 trapezoidal segments.

Discussion of Numerical Results

It is apparent from Table I that the 8 segment quadrupole fails to give an increase in the quadrupole strength at the bore as b/a decreases. The reason can be quickly traced to the rapid growth of ϕ_o as b/a decreases, with the resulting decrease in

the bore opening. This effect is somewhat reduced for 16 segments, where we have obtained a 5% increase in the quadrupole strength at the bore for b/a = .8, and further reduced for 32 segments, where an increase in the maximum quadrupole field of 11% is obtained near b/a = .7. Clearly, one needs a very large number of segments to approach the limiting increase of 18.5%.

The situation is similar for the elliptical dipole where, for 8 segments, the bore opening is significantly reduced. Nevertheless, for either segmented quadrupoles or dipoles, one has the opportunity to reduce the amount of REC significantly by using an elliptical design.

Other configurations are possible, and should be pursued according to the requirements of various applications. For example, one may keep all values of ϕ_j the same, and adjust the α_j for $j = 1, \ldots, \frac{N}{4} - 1$ to eliminate the multipoles $n = m+2, m+4, \ldots, m+\frac{N}{2}-2$. Clearly one has non-vanishing multipoles $n = m+\frac{N}{2}, m+\frac{N}{2}+2, \ldots, m+N-2$ compared with the circular case, but the field at the bore is larger and the segments are more nearly equal in size. Another option is to select the parameters (α_j, and possibly ϕ_j) to minimize the r.m.s. field at some intermediate radius. Still another option is to use non-touching segments. The preferred option should clearly be determined by the requirements of the application, i.e. overall field strength needed, multipole purity desired, useful aperture required, overall volume contraints, etc.

Table I
Elliptic Quadrupole with 8 segments

	b/a = 1.0			b/a = .8			b/a = .6		
j	ϕ_j	ψ_j	α_j	ϕ_j	ψ_j	α_j	ϕ_j	ψ_j	α_j
0	22.5°	0°	90°	33.33°	0°	90°	44.83°	0°	90°
1	22.5°	45°	225°	21.36°	54.69°	270.3°	17.90°	62.73°	307.5°
2	22.5°	90°	360°	14.95°	90°	360°	9.37°	90°	360°
$j^{(2)}$	1.537			1.470			1.238		

Table II
Elliptic Quadrupole with 16 Segments

	b/a = 1.0			b/a = .8			b/a = .6		
j	ϕ_j	ψ_j	α_j	ϕ_j	ψ_j	α_j	α_j	ψ_j	α_j
0	11.25°	0°	90°	17.79°	0°	90°	30.65°	0°	90°
1	11.25°	22.5°	157.5°	14.29°	32.08°	193.1°	15.02°	45.67°	247.1°
2	11.25°	45°	225°	9.98°	56.35°	263.0°	6.88°	67.57°	297.8°
3	11.25°	67.5°	292.5°	8.06°	74.39°	314.9°	5.32°	79.77°	331.4°
4	11.25°	90°	360°	7.54°	90°	360°	4.91°	90°	360°
$j^{(2)}$	1.875			1.974			1.810		

Summary

We have shown that a 2-D elliptical REC ring can be designed to produce a pure quadrupole or a pure dipole field, and that the limiting quadrupole field at the bore can be increased by a factor 32/27 over the circular ring for a major/minor axis ratio of 2. We have also obtained the multipole field spectrum for trapezoidal segments and developed a computer program which adjusts the easy axis orientation and segment angle openings to cause several of the unwanted multipole coefficients to vanish. Numerical results are presented which show that a large number of segments is needed to approach the results for the elliptical case.

References

[1] K. Halbach, LBL-8906 (1979); IEEE Trans. on Nuclear Science, June, 1979; Nucl. Instr. and Meth., 169 (1980) 1-10; R.F. Holsinger and K. Halbach, Proc. of 4th Intern. Workshop of Rare earth cobalts permanent magnets and their applications, Hakone National Park, Japan, May, 1979.

Table III
Elliptic Quadrupole with 32 Segments

	b/a = 1.0			b/a = .8			b/a = .6		
j	ϕ_j	ψ_j	α_j	ϕ_j	ψ_j	α_j	ϕ_j	ψ_j	α_j
0	5.63°	0°	90°	9.20°	0°	90°	18.92°	0°	90°
1	5.63°	11.25°	123.8°	8.48°	17.68°	144.5°	11.91°	30.83°	192.2°
2	5.63°	22.5°	157.5°	7.05°	33.21°	191.3°	6.31°	49.05°	240.8°
3	5.63°	33.75°	191.3°	5.81°	46.07°	229.5°	4.44°	59.80°	271.6°
4	5.63°	45°	225°	4.95°	56.83°	261.4°	3.49°	67.73°	294.6°
5	5.63°	56.25°	258.8°	4.38°	66.16°	289.1°	2.97°	74.19°	313.5°
6	5.63°	67.5°	292.5°	4.02°	74.56°	314.1°	2.67°	79.83°	330.0°
7	5.63°	78.75°	326.3°	3.83°	82.41°	337.4°	2.52°	85.02°	345.3°
8	5.63°	90°	360°	3.77°	90°	360°	2.47°	90°	360°
$j^{(2)}$	1.968			2.137			2.148		

Table IV
Elliptic Dipole with 8 Segments

	b/a = 1.0			b/a = .8			b/a = .6		
j	ϕ_j	ψ_j	α_j	ϕ_j	ψ_j	α_j	ϕ_j	ψ_j	α_j
0	22.5°	0°	90°	31.61°	0°	90°	44.05°	0°	90°
1	22.5°	45°	180°	21.40°	53.01°	204.7°	17.68°	61.93°	227.7°
2	22.5°	90°	270°	15.59°	90°	270°	10.19°	90°	270°
$j^{(1)}$	.900			.876			.794		

Table V
Elliptic Dipole with 16 Segments

	b/a = 1.0			b/a = .8			b/a = .6		
j	ϕ_j	ψ_j	α_j	ϕ_j	ψ_j	α_j	ϕ_j	ψ_j	α_j
0	11.25°	0°	90°	17.85°	0°	90°	30.90°	0°	90°
1	11.25°	22.5°	135°	14.19°	32.04°	157.6°	14.48°	45.38°	190.0°
2	11.25°	45°	180°	9.94°	56.17°	204.3°	7.06°	66.92°	226.2°
3	11.25°	67.5°	225°	8.13°	74.24°	239.3°	5.49°	79.47°	249.9°
4	11.25°	90°	270°	7.63°	90°	270°	5.05°	90°	270°
$j^{(1)}$	.975			.957			.891		